OPEN

Citation: Cell Death and Disease (2013) 4, e800; doi:10.1038/cddis.2013.322

www.nature.com/cddis

Interdigital cell death in the embryonic limb is associated with depletion of Reelin in the extracellular matrix

MJ Díaz-Mendoza[1], CI Lorda-Diez[1], JA Montero[1], JA García-Porrero[1] and JM Hurlé*[,1]

Interdigital cell death is a physiological regression process responsible for sculpturing the digits in the embryonic vertebrate limb. Changes in the intensity of this degenerative process account for the different patterns of interdigital webbing among vertebrate species. Here, we show that Reelin is present in the extracellular matrix of the interdigital mesoderm of chick and mouse embryos during the developmental stages of digit formation. Reelin is a large extracellular glycoprotein which has important functions in the developing nervous system, including neuronal survival; however, the significance of Reelin in other systems has received very little attention. We show that *reelin* expression becomes intensely downregulated in both the chick and mouse interdigits preceding the establishment of the areas of interdigital cell death. Furthermore, fibroblast growth factors, which are cell survival signals for the interdigital mesoderm, intensely upregulated *reelin* expression, while BMPs, which are proapototic signals, downregulate its expression in the interdigit. Gene silencing experiments of *reelin* gene or its intracellular effector *Dab-1* confirmed the implication of Reelin signaling as a survival factor for the limb undifferentiated mesoderm. We found that Reelin activates canonical survival pathways in the limb mesoderm involving protein kinase B and focal adhesion kinase. Our findings support that Reelin plays a role in interdigital cell death, and suggests that anoikis (apoptosis secondary to loss of cell adhesion) may be involved in this process.

Cell Death and Disease (2013) **4,** e800; doi:10.1038/cddis.2013.322; published online 12 September 2013
Subject Category: Experimental Medicine

In the developing vertebrate limb, the formation of free digits involves massive cell death within the interdigital mesoderm. These zones of cell death have been originally termed interdigital necrotic areas but constitute a classical example of physiological cell death by apoptosis.[1] Numerous studies have analyzed the molecular cascade activated in the course of the cell death process; however, the mechanisms triggering interdigital tissue regression remain controversial.[2–8] Local activation of bone morphogenetic protein (BMP) signaling, together with local downregulation of fibroblast growth factor (FGF) signaling, is central in the course of interdigital regression.[9–11] However, how these signals modify the interdigital tissue to initiate apoptosis is not fully understood. It has been proposed that modifications of the extracellular matrix[12] and loss of adhesion of the interdigital mesoderm to the surrounding extracellular matrix precedes the activation of intracellular apoptotic machinery.[4] This mechanism has been termed 'anoikis' and it occurs in both embryonic and tumoral cell death.[13,14] The identification of compositional changes in the interdigital matrix preceding the onset of cell death may be relevant for understanding the regulation of this degenerative process.

In a systematic analysis of a c-DNA library obtained from the undifferentiated interdigital mesoderm prior to the onset of interdigital necrotic zones (INZ), we identified the presence of the *reelin* gene.[15] Reelin is a large matrix glycoprotein thought to be expressed preferentially in the developing brain[16] where it controls the migration and laminar arrangement of neurons when the cerebral cortex is formed.[17] Remarkably, Reelin signaling also promotes the survival of different embryonic and adult neuronal populations.[18–20] In the developing neural system, Reelin binds to integrins[21–23] as well as specific receptors, including the very-low-density lipoprotein receptor (VLDLR) and apolipoprotein E receptor 2 (ApoER2) inducing the phosphorylation of the intracellular adaptor protein Disabled-1 (Dab-1),[24–26] which in turn activates downstream effectors involved in cytoskeletal reorganization, cell migration and cell survival.[27]

In this study, we show that Reelin and its intracellular signaling protein DAB-1 are highly expressed in the undifferentiated mesoderm during digit formation and are down-regulated in the interdigits preceding the onset of apoptosis. In accordance with a pro-survival role of this signaling pathway, *reelin* gene expression is upregulated *in vivo* by local treatment with FGFs which are survival signals for the interdigital mesoderm and down-regulated by BMPs which are pro-apoptotic signals. In addition, the knockdown of *reelin* or *Dab-1* by short hairpin RNA (sh-RNA) transfection

[1]Departamento de Anatomía y Biología Celular and IFIMAV, Facultad de Medicina, Universidad de Cantabria, Santander, 39011, Spain
*Corresponding author: JM Hurlé, Departamento de Anatomía y Biología Celular and IFIMAV, Facultad de Medicina, C/ Cardenal Herrera Oria s/n, Santander 39011, Spain. Tel: +34 942 201922; Fax: +34 942 201903; E-mail: hurlej@unican.es
Keywords: embryonic limb; apoptosis; disabled-1; progress zone; Syndactily; extracellular matrix
Abbreviations: FGFs, fibroblast growth factors; BMPs, bone morphogenetic proteins; TGFβ, transforming growth factor β; Dab-1, disabled-1; FAK, focal adhesion kinase; AKT, protein kinase B; ApoER2, apolipoprotein E receptor 2; PI3K, phosphatidylinositol-3-kinase; INZ, interdigital necrotic zones; AER, apical ectodermal ridge; PZ, progress zone; sh-RNA, short hairpin RNA; cDNA, complementary DNA; HH, Hamburger–Hamilton stages; i.d., incubation day; p.c., post-coitum; TUNEL, terminal deoxynucleotidyl transferase dUTP nick end labeling; DMEM, Dulbecco's modified Eagle's medium; PFA, paraformaldehyde; EDTA, ethylenediaminetetraacetic acid; SDS, sodium dodecyl sulfate; PBS, phosphate-buffered saline; AP, alkaline phosphatase; PI, propidium iodide
Received 17.4.13; revised 08.7.13; accepted 30.7.13; Edited by M Piacentini

increases cell death in primary cultures of the undifferentiated mesoderm. Finally, we identified focal adhesion kinase (FAK) and protein kinase B (AKT) as potential mediators of the pro-survival effect of Reelin signaling.

Results

***Reelin* and *Dab-1* are highly expressed in the undifferentiated mesoderm prior to the onset of INZ.** The *reelin* gene was identified in a complementary DNA (cDNA) library generated from the interdigital mesoderm of the developing chick limb in the stages preceding cell death.[15] We cloned *reelin* and used *in situ* hybridization to analyze its expression pattern during the formation of the digits in chick and mouse embryos. As shown in (Figures 1a and e), prior to INZ in the chick embryo, *reelin* exhibited intense expression domains in the undifferentiated mesoderm localized around the tip of the developing digits, as well as in the interdigital regions where cells are healthy and remain undifferentiated. In the following stages, interdigital expression was downregulated preceding the establishment of the areas of interdigital cell death that are responsible for digit freeing (Figures 1b and f). A gene expression analysis by Q-PCR was used to confirm the intense downregulation of *reelin* detected by *in situ* hybridization (Figure 1g). The presence of the Reelin protein

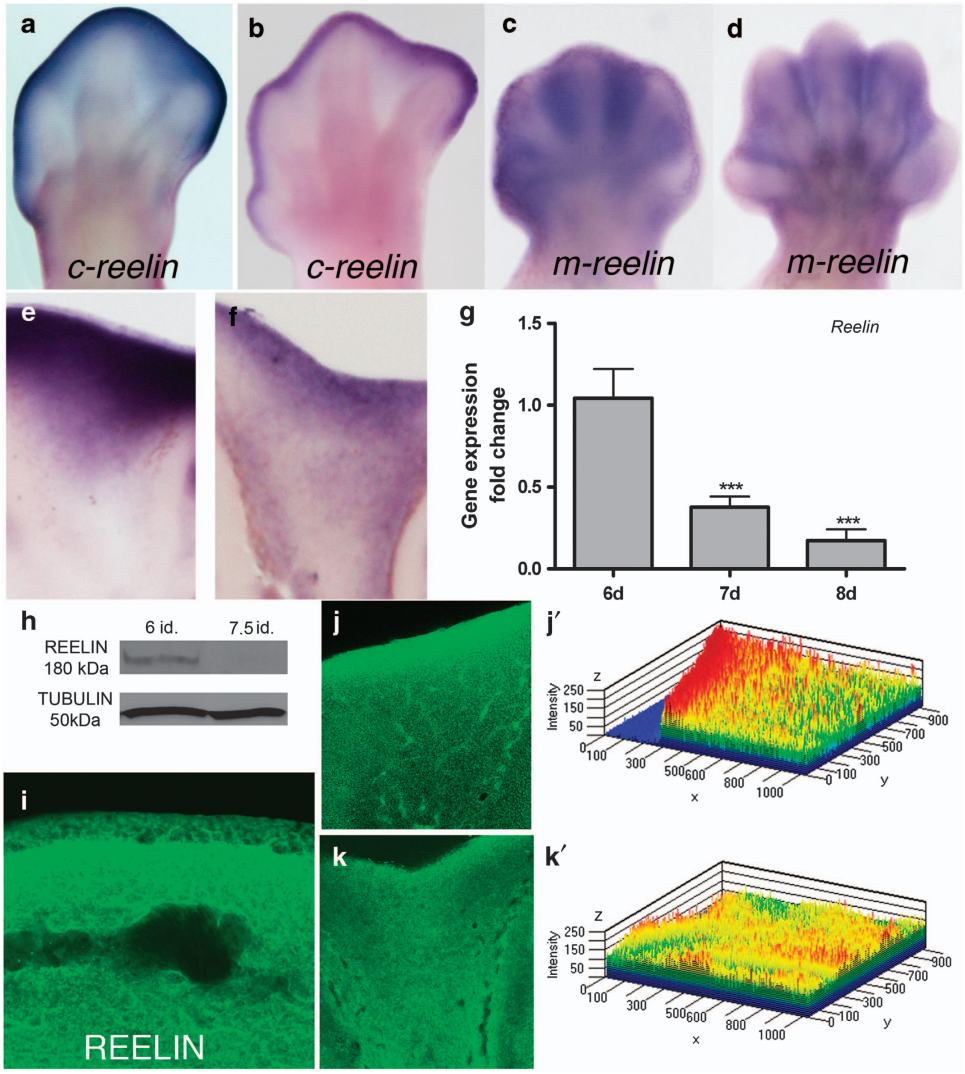

Figure 1 (**a** and **b**) *In situ* hybridization illustrating *reelin* expression in the developing chick autopod at 6 i.d. (**a**), and 7.5 i.d. (**b**). Prior to INZ (**a**) labeling is intense in the interdigital and distal undifferentiated mesoderm. From i.d. 7, interdigital expression is progressively downregulated (**b**). (**c** and **d**) *In situ* hybridization of mouse autopods prior to (p.c. day 12.5; **c**) and at the onset of (p.c. day 13.5; **d**) INZ. Note the intense labeling in the interdigital mesoderm in (**c**), and a weaker labeling in (**d**). (**e** and **f**) Detailed views of the third interdigit of chick leg buds to show differences in the intensity of *reelin* expression at 6 i.d. (**e**) and 7,5 i.d. (**f**). (**g**) QPCR analysis of *reelin* expression in the interdigital tissue of 6 i.d., 7 i.d. and 8 i.d. embryos. Bars represent gene expression levels in arbitrary units where values are normalized to the expression in the 6 i.d. tissue. $^{***}P<0.001$. (**h**) Representative western blot illustrating differences in Reelin levels in 6d *vs* 7.5d interdigital tissues. (**i**) Detailed view of a section of the chick autopod at 6 i.d. showing positive Reelin immunolabeling in the distal undifferentiated mesoderm. (**j** and **k**) Low-magnification views of the third interdigit at 6 i.d. (**j**), and 7.5 i.d. (**k**) immunostained for Reelin. (**j′** and **k′**) Surface plots quantifiying the distribution of Reelin immunolabeling in (**j** and **k**). z axes = counts of pixel intensity; x and y axes = pixel localization in the corresponding pictures (**j** and **k**). Red and green colors represent higher and lower values, respectively

in the autopodial tissues (Figure 1i) and its depletion preceding cell death (Figures 1 j–k) were also confirmed by western blotting (Figure 1h) and immunolabeling of autopodial vibratome sections monitored by confocal microscopy (Figures 1j–j′, k–k′). *Reelin* expression was also intense in the interdigits of mouse embryos on day 11 p.c. (Figure 1c). As observed in the chick, expression diminishes in the following stages in relation with the induction of INZ (Figure 1d). Remarkably, in contrast to what was observed in the chick embryo, *reelin* expression in the distal contour of the autopod was very low. This finding is consistent with the presence of an area of cell death termed 'Sub AER Marginal Zone of cell death' in the mouse autopod that is not present in avians.[29]

Reelin signaling is mediated by phosphorylation of the intracellular adaptor protein DAB-1 upon Reelin binding to its target receptors. Hence, to confirm that this signaling pathway is active during the stages of digit formation, we further analyzed the presence of Dab-1, both at transcriptional and protein level. As shown in Figure 2a, expression of *Dab-1* in the undifferentiated mesoderm overlaps with that of *reelin*. At protein level, DAB-1 exhibited a widespread distribution in the undifferentiated interdigital mesoderm (Figure 2b and d). Specific immunolabeling for phosphorylated DAB-1 (p-DAB-1) confirmed the presence of active signaling in a considerable number of undifferentiated mesodermal cells (Figure 2c).

Regulation of *reelin* gene expression by FGFs and BMPs. To analyze the possible functions of Reelin in the interdigital mesoderm, we studied *reelin* gene regulation by growth factors known to regulate interdigital cell death (Figure 3). As shown in Figure 3b, the interdigital expression domain of *reelin* was extended following FGF-2 overexpression in the undifferentiated limb mesoderm. This treatment has been shown to inhibit interdigital cell death by maintaining mesodermal cells in an undifferentiated state.[30] By contrast, interdigital overexpression of BMP7 (Figure 3c), which promotes interdigital cell death,[31] inhibited *reelin* expression.

The regulations modulated by FGF-2 and BMP-7 treatments were confirmed by Q-PCR (Figures 3b′ and c′) and altogether these results demonstrate that *reelin* expression is promoted by canonical limb mesenchymal cell survival factors while it is inhibited by canonical apoptotic inducing cytokines.

Reelin/Dab1 signaling regulates mesodermal cell survival via AKT and FAK. In light of the results described above, we next explored the function of Reelin signaling in programmed cell death. For this purpose, we designed and

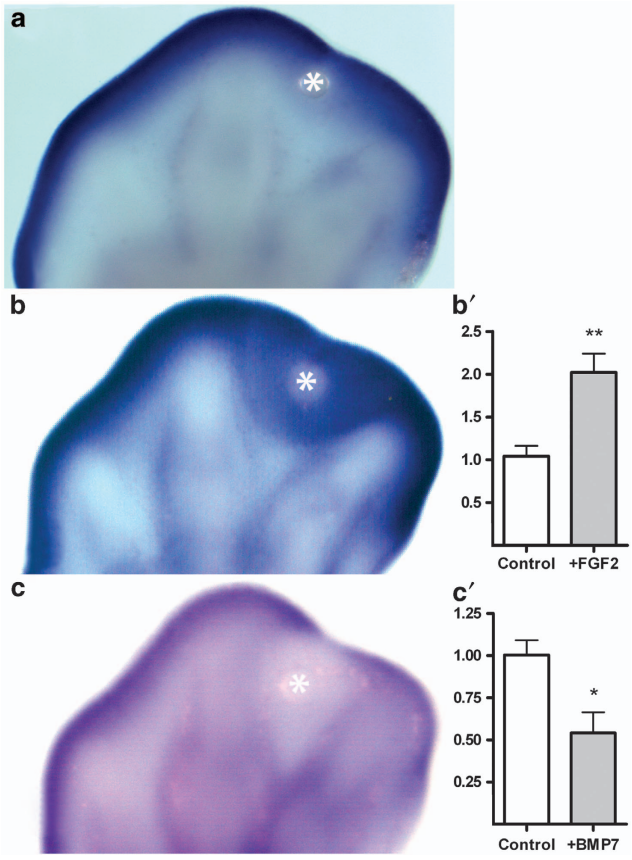

Figure 3 (**a–c**) Detailed view of *reelin* expression at 5.5 i.d., 6 h after interdigital implantation of PBS/BSA-soaked beads (**a**), FGF2-soaked beads (**b**), and BMP7-soaked beads (**c**). Note the upregulation of *reelin* expression in (**b**) and the downregulation in (**c**) in comparison to the control (**a**). Implanted bead is indicated by (*). (**b′**) QPCR plot showing the positive regulation of *reelin* in samples of the third interdigit isolated from the autopod 10 h after FGF-bead implantation. (**c′**) QPCR plots showing *reelin* downregulation in interdigit explants treated with BMP-7. $^{**}P<0.01$; $^{*}P<0.05$

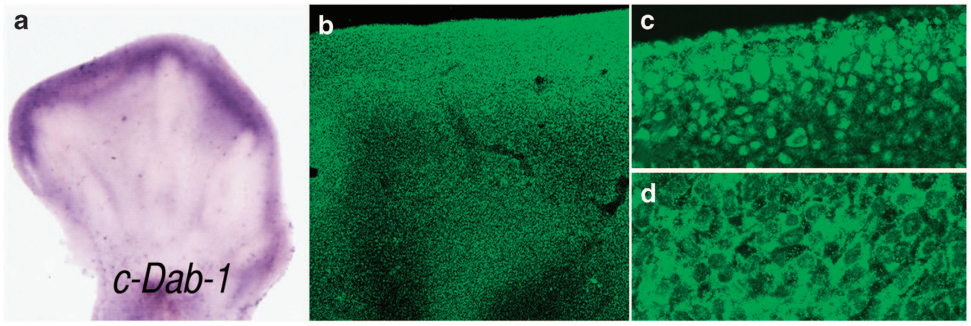

Figure 2 (**a**) *In situ* hybridization illustrating *Dab-1* expression in a vibratome section of the chick autopod at 7.5 i.d. Note that expression overlaps with that of *reelin* (**b**, in Figure 1). (**b**) Low-magnification view of the third interdigit at 6.5 i.d. immunolabeled with DAB-1. (**c** and **d**) Distal undifferentiated mesoderm at 6.5 i.d. showing p-DAB-1 (**c**) and non-phosphorylated DAB-1 (**d**) immunolabeling. Note that active signaling as revealed by p-DAB-1 predominates in the distal mesoderm

transfected *shReelin* or *shDab-1* constructs into undifferentiated mesodermal cells obtained from leg buds on days 4 and 5 of incubation (stage 26 HH). By Q-PCR and flow cytometry, we observed that the profile of gene regulation and cell death were similar after *reelin* or *Dab-1* silencing, although the effects of the latter were more intense. Hence, we used the *shDab-1* construct for subsequent studies. Changes in gene expression induced by *Dab-1* gene silencing (Figure 4) included downregulation of transforming growth factor β2 (*Tgfβ2*), which is a triggering signal for digit formation;[32] upregulation of *Glypican 3*, a cell surface anchored proteoglycan that inhibits cell proliferation and survival via interactions with several growth factors and adhesion and matrix molecules[33,34] and downregulation of *Snai1*, a transcription factor that regulates cell adhesion through the integrin signaling cascade.[35] The expression of other transcription factors characteristic of the undifferentiated and interdigital mesoderm including *Msx1* and *Snai2*/*Slug* were not modified.

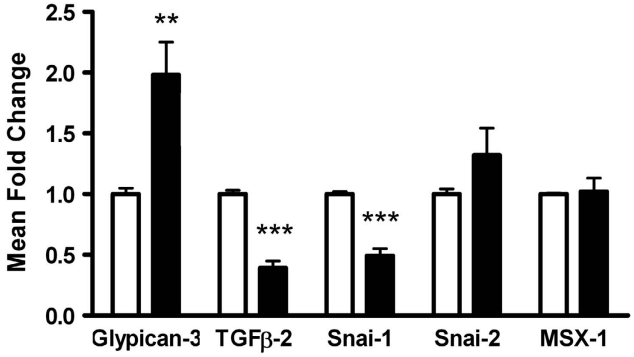

Figure 4 Chart showing the regulation of the *Glypican*, *Tgf β2*, *Msx-1*, *Snai-1*, and *Snai-2* genes in 3-day mesodermal cell cultures transfected with *shDab-1* (black column) in comparison to control cultures (white column). $^{***}P<0.001$; $^{**}P<0.01$

Changes in cell proliferation or cell death were analyzed by flow cytometry after propidium iodide (PI) staining. Proliferation was not modified in undifferentiated mesoderm that had been subjected to *Dab-1* silencing, but cell death increased significantly compared to control mesodermal cells transfected with the empty vector (Figures 5a–c). This increased cell death was confirmed by a terminal deoxynucleotidyl transferase dUTP nick end labeling (TUNEL) assay (Figures 5d–e). To further analyze whether cell death associated with *Dab-1* silencing recapitulates the regulatory mechanism responsible for physiological cell death in limb development, we analyzed the changes in protein kinase B (AKT). The maintenance of progress zone (PZ) mesoderm viability and proliferation is associated with the activation of AKT by phosphorylation.[36] We consistently detected more than 50% downregulation of AKT phosphorylation in mesodermal cells transfected with *shDab-1* (Figure 5f).

Because Reelin signaling is functionally associated with integrins,[21–23] the modification of gene expression after *Dab-1* silencing might well reflect changes in cell adhesion. We have

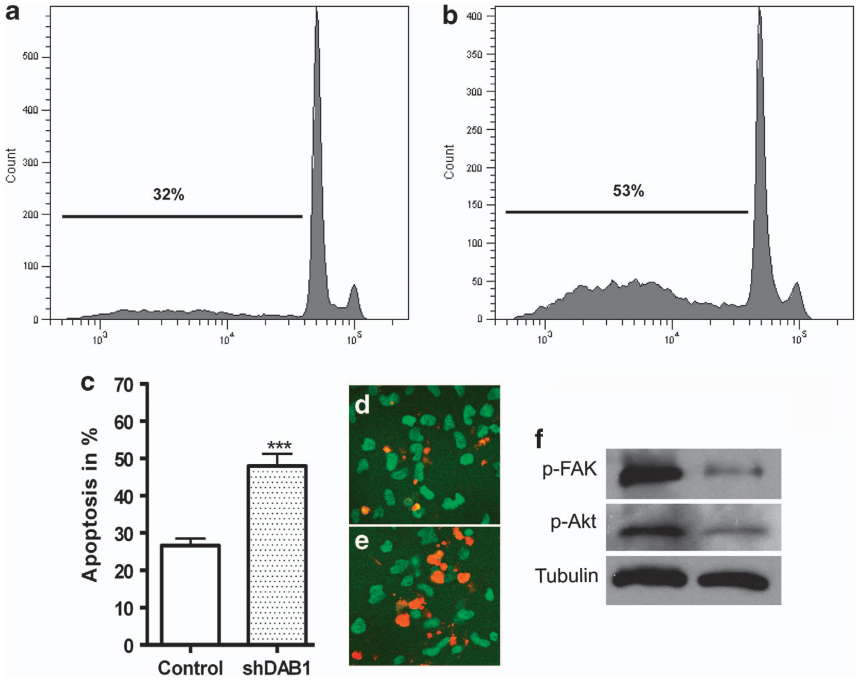

Figure 5 (**a**) Representative flow cytometry plots of dissociated propidium iodide-stained mesodermal cells indicating an increase in apoptosis in cells transfected with *shDab-1* (57% gene silencing), (**b**) in comparison to control cells transfected with the empty vector (A). (**c**) Average difference in the percentage of apoptotic cells in cells transfected with *sh-Dab-1* versus control cells as evaluated by flow cytometry ($^{***}P<0.001$). (**d** and **e**) Cell death analysis in undifferentiated limb mesodermal cells in controls (**d**) and upon *Dab-1* gene silencing (**e**) after immunolabeling for pan-histone (green) and TUNEL (red). (**f**) Western blot showing the inhibition of FAK and AKT phosphorylation in *Dab-1*-deficient cultures (right lane) in comparison to control cultures transfected with the empty vector (left lane)

previously shown that different integrins that are able to bind Reelin, including α3, α5, and β1, are expressed in the undifferentiated limb mesoderm.[37] Thus, we next explored changes in the integrin-dependent activation of focal adhesion kinase (FAK). As shown in Figure 5f, a 60 ± 8% reduction in phospho-FAK levels was observed by western blotting of samples obtained from *Dab-1* deficient mesodermal precursors.

Discussion

From the pioneering study of Saunders *et al.*,[38] which was later confirmed by modern molecular approaches,[39] it is known that the population of mesodermal cells occupying the distal tip of the limb, known as the PZ, is responsible for distal limb outgrowth. Mesodermal cells within this region are connective tissue progenitors and are maintained in an undifferentiated and proliferative state due to the influence of the apical ectodermal ridge (AER) rimming the distal margin of the bud. Cells undergo differentiation as they move out of the range of AER signaling. It has been shown that progress zone progenitors require survival factors until they initiate differentiation.[40,41] Consistent with these observations, when digit primordia are formed, undifferentiated cells that occupy the interdigital spaces suffer massive apoptosis that sculpt the digits from the hand and foot plates. FGFs produced by the AER are considered major survival signals for the undifferentiated limb mesoderm,[30] while BMPs exert an opposing function that promotes cell death.[31] Here, we show that Reelin signaling is active in the undifferentiated mesoderm and is downregulated preceding the regression of interdigital tissue in chick and mouse embryos.

Reelin is a large extracellular matrix glycoprotein with putative functions in the embryonic and adult nervous systems; however, increasing information shows that Reelin is also implicated in other systems.[42–46] Our findings suggest that Reelin contributes to the creation of an extracellular substrate required for maintaining the viability of undifferentiated limb mesodermal cells until they initiate differentiation. In chick limbs, the interdigital expression of *reelin* is intensely downregulated preceding cell death. Moreover, we observed that *reelin* is upregulated by a local application of FGFs. These treatments cause the inhibition of interdigital cell death.[30] In a complementary fashion, local application of BMPs, which are proapototic factors,[47] downregulates the expression of *reelin*. Consistent with these findings, disruption of Reelin signaling by silencing *Dab-1* increases apoptosis. Markers of the undifferentiated mesoderm such as *Msx1* and *Snai2/Slug* were not regulated. However, the zinc-finger transcription factor *Snai1*,[48] which shows the same interdigital expression pattern as *reelin* and *Dab-1* in the autopod,[30] was significantly downregulated. *Snai1* contributes to the maintenance of the immature phenotype of stem cells and regulates cell adhesion in the integrin signaling cascade.[35]

Dab-1 is a central component of Reelin signaling. It is phosphorylated by Src family of non-receptor tyrosine kinases[26,27] after binding of Reelin to its target receptors. Phosphorylated DAB-1 activates intracellular kinases, including Src, phosphatidylinositol-3-kinase (PI3K), the serine/threonine kinase AKT, and the mitogen-activated protein kinase/extracellular signal-regulated kinase, Erk.[25,49,50] Although the activity of phosphorylated DAB-1 has been largely associated with the stabilization of the cytoskeleton and regulation of neuronal migration (reviewed by Herz and Chen[51]), there is evidence that suggest that some of the neural functions of Reelin are due to the regulation of cell–matrix adhesion via binding to α3β1 integrin[22,23] or activation α5β1 integrin through a biologically conserved inside-out signaling cascade.[52] In our study, the transcriptional effects of *Dab-1* silencing are associated with reduced AKT and FAK phosphorylation, supporting a role for Reelin/Dab-1 signaling in the promotion of cell–matrix adhesion via integrins. FAK is a major downstream effector of integrin signaling and is implicated in the formation of the prechondrogenic aggregates.[53–55] Furthermore, the activation of AKT accounts for the pro-survival influence of FGFs in the developing limb.[36] Both FAK and AKT have been identified as key targets of cell death by anoikis.[56] Together, these findings suggest that the disruption of Reelin signaling in the mesodermal tissue is followed by reduced integrin-mediated cell adhesion. Many different integrins, including α3, α5, and β1, are expressed in digit progenitors.[37] Integrins recognize various extracellular matrix components that are abundant in the developing limb, and deficiencies in some of these components are associated with syndactylous mice phenotypes.[57,58] This fact makes it difficult to establish the relative importance of Reelin in the regression of the interdigital tissue. Mice deficient in *reelin* or *Dab-1* (Reeler or Yotari mutants, respectively) lack the syndactylous phenotype,[59] suggesting functional redundancy of Reelin with other matrix molecules present in the embryonic limb. In addition, it must be taken into account that the absence of Reelin in mice mutants occurs through the entire embryonic development and not in a small window of time analyzed in our *in vitro* experiments. Furthermore, predicting protein-protein interactions by a computational algorithm based on structural, functional, and evolutionary data (http://bhapp.c2b2.columbia.edu/PrePPI[60]) identifies more than 100 matrix and regulatory molecules expressed in the developing limb that are likely to interact with Reelin. Our findings, together with these observations, suggest that Reelin, while not strictly necessary, contributes to sustain the anchoring of the undifferentiated mesoderm to the extracellular matrix to prevent anoikis.

Materials and Methods

In this work, we employed Rhode Island chicken embryos from 4.5 to 8 days of incubation (i.d.), which were equivalent to stages 25 to 36 HH and C57BL6 mouse embryos ranging from 11 to 14 days *post coitum* (p.c.).

***In situ* hybridization.** *In situ* hybridization was performed in whole-mount specimens and vibratome tissue sections. Samples fixed in 4% paraformaldehyde (PFA) were treated with 10 μg/ml of proteinase K for 20–30 min at 20 °C. Hybridization with digoxigenin-labeled antisense RNA probes was performed at 68 °C. Alkaline phosphatase-conjugated anti-digoxigenin antibody (dilution 1:2000) was used (Roche Applied Science, Indianapolis, IN, USA). Reactions were developed with the BM Purple AP Substrate precipitating solution (Roche Applied Science).

The probes for *reelin* and *Dab-1* were obtained by PCR: chick Reelin 5′-CCTAACAATCGCAACCAAGG-3′ and 5′-AGCCTTCTGTTGGAGTCAGG-3′; for mouse *reelin* 5′-AACACAGTCCATGCAGATCG-3′ and 5′-CTTCCTGCCA GTCTGATTCC-3′; for chick *Dab-1* 5′-AACCTGTGATTCTGGACTTGC-3′ and 5′-TGAACAAGTGGTTGCTGTCC-3′.

In vivo gene regulation analysis was performed in the embryonic chick by whole-mount *in situ* hybridization following interdigital implantation at 5.5 i.d. of heparin beads (Sigma-Aldrich, St Louis, MO, USA) incubated for 1 h in 0.5 mg/ml FGF2 (PeproTech, Rocky Hill, NJ, USA) or 0.5 mg/ml BMP-7 (R&D Systems, Minneapolis, MN, USA). The contralateral left limb or limbs treated with beads incubated in phosphate-buffered saline (PBS) were used as controls. After manipulation, the eggs were sealed and further incubated until processing.

Mesodermal cultures. Undifferentiated mesodermal cells obtained from the region located under the AER of chick leg buds at 4.5 i.d. (25 HH) were suspended in medium DMEM (Dulbecco's modified Eagle's medium) with 10% fetal bovine serum, 100 units/ml penicillin and 100 μg/ml streptomycin. Cells were seeded on fibronectin-coated coverglasses and were grown as monolayers or cultured at a high density as micromass cultures.

Micromass cultures were made by pipetting 10-μl drops of cell suspension at a density of 2.0×10^7 cells/ml into each well of a 24-well plate. The cells were left to attach for 2 h and then 200 μl serum-free medium was added.

Micromasses were used to analyze cell proliferation and cell death in mesodermal cells subjected to *reelin* signaling knockdown. Monolayer cultures were used for TUNEL assay to detect cell death.

Quantitative analysis of *reelin* regulation by BMPs was performed in interdigital explants cultured for 5 h in presence of 0.6 μg/ml of BMP7.

Immunolabeling and TUNEL assay. Samples were fixed with 4% PFA O/N at 4 °C, washed with 0.1%Triton/PBS and incubated O/N at 4 °C with the primary antibody. Specimens were next washed with PBS, incubated O/N with the secondary antibody, washed for 2 h with PBS, dehydrated and cleared. Anti-Reelin (SC-5578, Santa Cruz Biotechnologies, Santa Cruz, CA, USA), anti-phospho-DAB-1 (SC-133292, Santa Cruz Biotechnologies) and anti-Dab1 (SC-7827, Santa Cruz Biotechnologies) polyclonal antibodies were used.

Samples were monitored by confocal microscopy, and analysis of immunolabeling intensity was performed measuring pixel intensity distribution using the LSM 5 Image Examiner software (LSM Software Zeiss, Oberkochen, Germany).

TUNEL was performed using the *in situ* cell death detection kit (Roche Applied Science) according to the manufacturer's instructions.

Cell nucleofection and target gene silencing. Functional studies were performed in chick embryos by a loss-of-function approach. For this purpose, limb mesodermal cells were transfected with a short hairpin RNAi for *reelin* (*shreelin*) or *Dab-1* (*shDab-1*) and cloned into the pcU6-1-shRNA (a generous gift of Dr Tim J Doran) as described by Wise *et al*.[28] The level of gene silencing was evaluated by Q-PCR and samples with a reduction in gene expression ranging between 45% and 60% were selected for further studies. Control transfections using a chU6-1v irrelevant control plasmid were performed in all experiments.

Western blot. For western blot analysis, total protein extracts were obtained from control and *shDab-1* silenced mesodermal cultures or interdigital tissues at different stages. Cell lysis was performed with RIPA buffer (150 mM NaCl, 1.5 mM $MgCl_2$, 10 mM NaF, 10% glycerol, 4 mM ethylenediaminetetraacetic acid (EDTA), 1% Triton X-100, 0.1% sodium dodecyl sulfate (SDS), 1% deoxycholate and 50 mM Hepes, pH 7.4) supplemented with the protease inhibitors phenylmethylsulfonyl fluoride (PMSF, 1 mM), leupetin (10 μg/ml) and aprotinin (10 μg/ml), for 15 min on ice. The cell lysates were clarified of cellular debris by centrifugation ($13\,200 \times g$) for 10 min at 4 °C. Proteins were separated by 8–10% polyacrilamide gel electrophoresis containing 0.1% SDS and transferred to nitrocellulose membrane (Protan; Whatman, Dassel, Germany). The membranes were incubated for 1 h at room temperature in bovine serum albumin and incubated overnight with the following antibodies: rabbit polyclonal antibody anti-phospho-Akt (SC-1011629, Santa Cruz Biotechnologies), anti-Reelin (SC-5578, Santa Cruz Biotechnologies) and anti-phospho-FAK Y576 (Abcam, Cambridge, UK; ab-4815), and mouse polyclonal antibody anti-tubulin (Sigma-Aldrich, T5168). Protein bands were detected in the membranes with an ODYSSEY infrared-imaging system (LI-COR Biosciences, Lincoln, NE, USA) according to ODYSSEY western blot protocol. Immunoblots were monitored using anti-mouse IRDye 800DX or anti-rabbit IRDye 680DX (Rockland Immunochemicals, Inc., Gilbertsville, PA, USA). The public domain image analysis program 'ImageJ' was employed to perform quantitative analysis.

Flow cytometry. Cell proliferation and cell death was deduced from measurement of DNA content by flow cytometry. Control and *shreelin* or *shDab-1* silenced cultures were dissociated to single-cell level by treatment with Trypsin EDTA (Lonza, Basel, Switzerland). One million cells were used in each test. For PI staining, the cells were washed twice in PBS and centrifuged at $405 \times g$ for 5 min at 4 °C. The samples were then incubated overnight at 4 °C with 0.1% sodium citrate, 0.01% Triton X-100 and 0.1 mg/ml PI. Cell suspension was subjected to flow cytometry analysis in a Becton Dickinson FacsCanto cytometer (BD Biosciences, San Jose, CA, USA) and analyzed with Cell Quest software (BD Biosciences). This technique allows the quantification of apoptotic (hypodiploid) and proliferating (hyperdiploid) cells according to their DNA content deduced from PI staining.

Real time quantitative PCR (Q-PCR) for gene expression analysis. Total RNA was extracted and cleaned from specimens using the RNeasy Mini Kit (Qiagen, Hilden, Germany). RNA samples were quantified using a spectrophotometer (NanoDrop Technologies, Wilmington, DE, USA). First-strand cDNA was synthesized by reverse transcription-PCR (RT-PCR) using random hexamers, and M-MulV reverse transcriptase (Fermentas GmbH, St Leon-Rot, Germany). The cDNA concentration was measured in a spectrophotometer (NanoDrop Technologies) and adjusted to 0.5 μg/μl. Q-PCR was performed using the Mx3005P system (Stratagene Inc., La Jolla, CA, USA) with automation attachment. In this work, we have used SYBRGreen (TaKaRa Inc., Otsu, Japan) based Q-PCR. *Gapdh* had no significant variation in expression across the sample set and therefore was chosen as the normalizer in our experiments. Mean values for fold changes were calculated for each gene. Expression level was evaluated relative to a calibrator according to the $2^{-(\Delta\Delta Ct)}$ equation. Each value in this work represents the mean ± standard error of the mean of at least three independent samples obtained under the same conditions. Samples consisted of 4 micromass cultures or 20 interdigital spaces. Data were analyzed using one-way analysis of variance followed by Bonferroni tests for post-hoc comparisons for gene expression levels in treated micromass cultures and Student's *t* test for gene expression levels in overexpression and silencing experiments. Statistical significance was set at $P < 0.05$. All the analyses were done using SPSS for Windows version 18.0. Q-PCR specific primers for chick genes were: for *Glypican 3* 5′-GGAGAAGTACCAGGCAGTGG-3′ and 5′-CAGCATTCTGGATGACAAGG-3′; for *Tgfβ2* 5′-TGCACTGCTATCTCCTGAGC-3′ and 5′-GCATGAACTGATCCA TGTCG-3′; for *Msx1* 5′-CAAGCACAAGACCAACAGGA-3′ and 5′-TACTGCT TCTGGCGGAATTT-3′; for *Snai2/Slug* 5′-ATACCGCAGCCAGAGATCC-3′ and 5′-AGCGGAGAGAGGTCATTGG-3′; for *Snai1/Snail* 5′-TGCGAGAAGGAGTA TGTGAGC-3′ and 5′-GCACATCTTGCAGACACAGG-3′; for *reelin* 5′-GCACAGT GACAGCATCATCC-3′ and 5′-GCTCTCCAATCTCACAGTTGC-3′; for *Dab1* 5′-AACCTGTGATTCTGGACTTGC-3′ and 5′-ATACCGCCTGTTCACACTGC-3′.

Conflict of Interest

The authors declare no conflict of interest.

Acknowledgements. We would like to thank Montse Fernandez-Calderon, Sonia Perez-Mantecón and Susana Dawalibi for excellent technical assistance. Thanks are also due to Drs Eduardo Soriano Lluis Pujadas and Ana Illundain for reagents and advice. This work was supported by a grant from the Spanish Ministry of Economy and Competitiveness to JMH (BFU2011-24169). M J D-M is a recipient of a predoctoral FPI fellowship from the Spanish Ministry of Economy and Competitiveness.

1. Garcia-Martinez V, Macias D, Ganan Y, Garcia-Lobo JM, Francia MV, Fernandez-Teran MA *et al*. Internucleosomal DNA fragmentation and programmed cell death (apoptosis) in the interdigital tissue of the embryonic chick leg bud. *J Cell Sci* 1993; **106**(Pt 1): 201–208.
2. Arteaga-Solis E, Gayraud B, Lee SY, Shum L, Sakai L, Ramirez F. Regulation of limb patterning by extracellular microfibrils. *J Cell Biol* 2001; **154**: 275–281.
3. Rodriguez-Leon J, Merino R, Macias D, Ganan Y, Santesteban E, Hurle JM. Retinoic acid regulates programmed cell death through BMP signalling. *Nat. Cell Biol* 1999; **1**: 125–126.
4. Zuzarte-Luis V, Berciano MT, Lafarga M, Hurle JM. Caspase redundancy and release of mitochondrial apoptotic factors characterize interdigital apoptosis. *Apoptosis* 2006; **11**: 701–715.
5. Montero JA, Lorda-Diez CI, Certal AC, Moreno N, Rodriguez-Leon J, Torriglia A *et al*. Coordinated and sequential activation of neutral and acidic DNases during interdigital cell death in the embryonic limb. *Apoptosis* 2010; **15**: 1197–1210.

6. Ren D, Tu HC, Kim H, Wang GX, Bean GR, Takeuchi O *et al.* BID, BIM, and PUMA are essential for activation of the BAX- and BAK-dependent cell death program. *Science* 2010; **330**: 1390–1393.
7. Hernandez-Martinez R, Covarrubias L. Interdigital cell death function and regulation: new insights on an old programmed cell death model. *Dev. Growth Differ* 2011; **53**: 245–258.
8. Aizawa R, Yamada A, Suzuki D, Iimura T, Kassai H, Harada T *et al.* Cdc42 is required for chondrogenesis and interdigital programmed cell death during limb development. *Mech Dev* 2012; **129**: 38–50.
9. Zou H, Niswander L. Requirement for BMP signaling in interdigital apoptosis and scale formation. *Science* 1996; **272**: 738–741.
10. Hernandez-Martinez R, Castro-Obregon S, Covarrubias L. Progressive interdigital cell death: regulation by the antagonistic interaction between fibroblast growth factor 8 and retinoic acid. *Development* 2009; **136**: 3669–3678.
11. Wong YL, Behringer RR, Kwan KM. Smad1/Smad5 signaling in limb ectoderm functions redundantly and is required for interdigital programmed cell death. *Dev Biol* 2012; **363**: 247–257.
12. McCulloch DR, Nelson CM, Dixon LJ, Silver DL, Wylie JD, Lindner V *et al.* ADAMTS metalloproteases generate active versican fragments that regulate interdigital web regression. *Dev Cell* 2009; **17**: 687–698.
13. Grossmann J, Walther K, Artinger M, Kiessling S, Scholmerich J. Apoptotic signaling during initiation of detachment-induced apoptosis ("anoikis") of primary human intestinal epithelial cells. *Cell Growth Differ* 2001; **12**: 147–155.
14. Ioannides AS, Massa V, Ferraro E, Cecconi F, Spitz L, Henderson DJ *et al.* Foregut separation and tracheo-oesophageal malformations: the role of tracheal outgrowth, dorso-ventral patterning and programmed cell death. *Dev Biol* 2010; **337**: 351–362.
15. Zuzarte-Luis V, Montero JA, Rodriguez-Leon J, Merino R, Rodriguez-Rey JC, Hurle JM. A new role for BMP5 during limb development acting through the synergic activation of Smad and MAPK pathways. *Dev Biol* 2004; **272**: 39–52.
16. D'Arcangelo G, Nakajima K, Miyata T, Ogawa M, Mikoshiba K, Curran T. Reelin is a secreted glycoprotein recognized by the CR-50 monoclonal antibody. *J Neurosci* 1997; **17**: 23–31.
17. Soriano E, Del Rio JA. The cells of cajal-retzius: still a mystery one century after. *Neuron* 2005; **46**: 389–394.
18. Beffert U, Nematollah Farsian F, Masiulis I, Hammer RE, Yoon SO, Giehl KM *et al.* ApoE receptor 2 controls neuronal survival in the adult brain. *Curr Biol* 2006; **16**: 2446–2452.
19. Ohkubo N, Vitek MP, Morishima A, Suzuki Y, Miki T, Maeda N *et al.* Reelin signals survival through Src-family kinases that inactivate BAD activity. *J Neurochem* 2007; **103**: 820–830.
20. Peterziel H, Sackmann T, Strelau J, Kuhn PH, Lichtenthaler SF, Marom K *et al.* F-spondin regulates neuronal survival through activation of disabled-1 in the chicken ciliary ganglion. *Mol. Cell. Neurosci* 2011; **46**: 483–497.
21. Sanada K, Gupta A, Tsai LH. Disabled-1-regulated adhesion of migrating neurons to radial glial fiber contributes to neuronal positioning during early corticogenesis. *Neuron* 2004; **42**: 197–211.
22. Dulabon L, Olson EC, Taglienti MG, Eisenhuth S, McGrath B, Walsh CA *et al.* Reelin binds alpha3beta1 integrin and inhibits neuronal migration. *Neuron* 2000; **27**: 33–44.
23. Schmid RS, Jo R, Shelton S, Kreidberg JA, Anton ES. Reelin, integrin and DAB1 interactions during embryonic cerebral cortical development. *Cereb Cortex* 2005; **15**: 1632–1636.
24. Arnaud L, Ballif BA, Forster E, Cooper JA. Fyn tyrosine kinase is a critical regulator of disabled-1 during brain development. *Curr. Biol* 2003; **13**: 9–17.
25. Bock HH, Herz J. Reelin activates SRC family tyrosine kinases in neurons. *Curr Biol* 2003; **13**: 18–26.
26. Kuo G, Arnaud L, Kronstad-O'Brien P, Cooper JA. Absence of Fyn and Src causes a reeler-like phenotype. *J. Neurosci* 2005; **25**: 8578–8586.
27. Frotscher M, Chai X, Bock HH, Haas CA, Forster E, Zhao S. Role of Reelin in the development and maintenance of cortical lamination. *J Neural Transm* 2009; **116**: 1451–1455.
28. Wise TG, Schafer DJ, Lambeth LS, Tyack SG, Bruce MP, Moore RJ *et al.* Characterization and comparison of chicken U6 promoters for the expression of short hairpin RNAs. *Anim Biotechnol* 2007; **18**: 153–162.
29. Fernandez-Teran MA, Hinchliffe JR, Ros MA. Birth and death of cells in limb development: a mapping study. *Dev Dyn* 2006; **235**: 2521–2537.
30. Montero JA, Ganan Y, Macias D, Rodriguez-Leon J, Sanz-Ezquerro JJ, Merino R *et al.* Role of FGFs in the control of programmed cell death during limb development. *Development* 2001; **128**: 2075–2084.
31. Macias D, Ganan Y, Sampath TK, Piedra ME, Ros MA, Hurle JM. Role of BMP-2 and OP-1 (BMP-7) in programmed cell death and skeletogenesis during chick limb development. *Development* 1997; **124**: 1109–1117.
32. Merino R, Ganan Y, Macias D, Economides AN, Sampath KT, Hurle JM. Morphogenesis of digits in the avian limb is controlled by FGFs, TGFbetas, and noggin through BMP signaling. *Dev Biol* 1998; **200**: 35–45.
33. De Cat B, Muyldermans SY, Coomans C, Degeest G, Vanderschueren B, Creemers J *et al.* Processing by proprotein convertases is required for glypican-3 modulation of cell survival, Wnt signaling, and gastrulation movements. *J Cell Biol* 2003; **163**: 625–635.
34. Hartwig S, Hu MC, Cella C, Piscione T, Filmus J, Rosenblum ND. Glypican-3 modulates inhibitory Bmp2-Smad signaling to control renal development in vivo. *Mech Dev* 2005; **122**: 928–938.
35. Wu Y, Zhou BP. Snail: More than EMT. *Cell. Adh Migr* 2010; **4**: 199–203.
36. Kawakami Y, Rodriguez-Leon J, Koth CM, Buscher D, Itoh T, Raya A *et al.* MKP3 mediates the cellular response to FGF8 signalling in the vertebrate limb. *Nat Cell Biol* 2003; **5**: 513–519.
37. Lorda-Diez CI, Montero JA, Diaz-Mendoza MJ, Garcia-Porrero JA, Hurle JM. Defining the earliest transcriptional steps of chondrogenic progenitor specification during the formation of the digits in the embryonic limb. *PLoS One* 2011; **6**: e24546.
38. Saunders JW Jr.. The proximo-distal sequence of origin of the parts of the chick wing and the role of the ectoderm. 1948. *J Exp Zool* 1998; **282**: 628–668.
39. Tabin C, Wolpert L. Rethinking the proximodistal axis of the vertebrate limb in the molecular era. *Genes Dev* 2007; **21**: 1433–1442.
40. Rowe DA, Fallon JF. The proximodistal determination of skeletal parts in the developing chick leg. *J Embryol Exp Morphol* 1982; **68**: 1–7.
41. Dudley AT, Ros MA, Tabin CJ. A re-examination of proximodistal patterning during vertebrate limb development. *Nature* 2002; **418**: 539–544.
42. Maurin JC, Couble ML, Didier-Bazes M, Brisson C, Magloire H, Bleicher F. Expression and localization of reelin in human odontoblasts. *Matrix Biol* 2004; **23**: 277–285.
43. Sato N, Fukushima N, Chang R, Matsubayashi H, Goggins M. Differential and epigenetic gene expression profiling identifies frequent disruption of the RELN pathway in pancreatic cancers. *Gastroenterology* 2006; **130**: 548–565.
44. Khialeeva E, Lane TF, Carpenter EM. Disruption of reelin signaling alters mammary gland morphogenesis. *Development* 2011; **138**: 767–776.
45. Yuan Y, Chen H, Ma G, Cao X, Liu Z. Reelin is involved in transforming growth factor-beta1-induced cell migration in esophageal carcinoma cells. *PLoS One* 2012; **7**: e31802.
46. Garcia-Miranda P, Vazquez-Carretero MD, Sesma P, Peral MJ, Ilundain AA. Reelin is involved in the crypt-villus unit homeostasis. *Tissue Eng* Part A 2013; **19**: 188–198.
47. Zuzarte-Luis V, Hurle JM. Programmed cell death in the embryonic vertebrate limb. *Semin Cell Dev Biol* 2005; **16**: 261–269.
48. Barrallo-Gimeno A, Nieto MA. The Snail genes as inducers of cell movement and survival: implications in development and cancer. *Development* 2005; **132**: 3151–3161.
49. Beffert U, Morfini G, Bock HH, Reyna H, Brady ST, Herz J. Reelin-mediated signaling locally regulates protein kinase B/Akt and glycogen synthase kinase 3beta. *J Biol Chem* 2002; **277**: 49958–49964.
50. Simo S, Pujadas L, Segura MF, La Torre A, Del Rio JA, Urena JM *et al.* Reelin induces the detachment of postnatal subventricular zone cells and the expression of the Egr-1 through Erk1/2 activation. *Cereb Cortex* 2007; **17**: 294–303.
51. Herz J, Chen Y. Reelin. lipoprotein receptors and synaptic plasticity. *Nat Rev Neurosci* 2006; **7**: 850–859.
52. Sekine K, Kawauchi T, Kubo K, Honda T, Herz J, Hattori M *et al.* Reelin controls neuronal positioning by promoting cell-matrix adhesion via inside-out activation of integrin alpha5beta1. *Neuron* 2012; **76**: 353–369.
53. Bang OS, Kim EJ, Chung JG, Lee SR, Park TK, Kang SS. Association of focal adhesion kinase with fibronectin and paxillin is required for precartilage condensation of chick mesenchymal cells. Biochem. *Biophys Res Commun* 2000; **278**: 522–529.
54. Choi YA, Kim DK, Kang SS, Sonn JK, Jin EJ. Integrin signaling and cell spreading alterations by rottlerin treatment of chick limb bud mesenchymal cells. *Biochimie* 2009; **91**: 624–631.
55. Rokutanda S, Fujita T, Kanatani N, Yoshida CA, Komori H, Liu W *et al.* Akt regulates skeletal development through GSK3, mTOR, and FoxOs. *Dev Biol* 2009; **328**: 78–93.
56. Zheng Y, Gierut J, Wang Z, Miao J, Asara JM, Tyner AL. Protein tyrosine kinase 6 protects cells from anoikis by directly phosphorylating focal adhesion kinase and activating AKT. *Oncogene* 2012; e-pub ahead of print 1 October 2012; doi:10.1038/onc.2012.427.
57. Miner JH, Cunningham J, Sanes JR. Roles for laminin in embryogenesis: exencephaly, syndactyly, and placentopathy in mice lacking the laminin alpha5 chain. *J Cell Biol* 1998; **143**: 1713–1723.
58. Bose K, Nischt R, Page A, Bader BL, Paulsson M, Smyth N. Loss of nidogen-1 and -2 results in syndactyly and changes in limb development. *J Biol Chem* 2006; **281**: 39620–39629.
59. Katsuyama Y, Terashima T. Developmental anatomy of reeler mutant mouse. *Dev Growth Differ* 2009; **51**: 271–286.
60. Zhang QC, Petrey D, Garzon JI, Deng L, Honig B. PrePPI: a structure-informed database of protein-protein interactions. *Nucleic Acids Res* 2013; **41**: D828–D833.